Part II Applied Physics

Section 1 Atomic, Molecular and Optical Physics

Chapter 1. Quantum Optics and Photonics

Academic and Research Staff

Professor Shaoul Ezekiel

Visiting Scientists and Research Affiliates

Dr. Philip R. Hemmer, John D. Kierstead, Dr. Elias Snitzer,[1] Dr. Mara G. Prentiss[2]

Graduate Students

M. Selim Shahriar, Stephen P. Smith, Farhad Zarinetchi, John J. Donoghue

Technical and Support Staff

Margaret M. McCabe

1.1 Applications of Stimulated Brillouin Fiber Lasers

Sponsor

Charles S. Draper Laboratory
Contract DL-H-418468

Brillouin scattering,[3] i.e., spontaneous Brillouin scattering, is the scattering of an incident field, the pump, by thermal acoustic waves in the medium, or, fiber, in our case. Of interest here is the scattering by acoustic waves propagating along the fiber. Since forward scattering by such acoustic waves does not generate a frequency shifted beam, it has no interest for us. However, backscattering by such acoustic waves will generate a beam that is doppler shifted by $2 f_p v_a/c_m$ from the pump, where f_p is the frequency of the pump, v_a is the acoustic velocity in the fiber, and c_m is the speed of light in the fiber medium. The peak amplitude of the backscattered wave, frequency f_B, is derived from that acoustic wave that satisfies the Bragg condition, i.e., $2\lambda_a = \lambda_{Bm}$, where λ_a is the wavelength of that acoustic wave, and λ_{Bm} is the wavelength of the backscattered wave in the medium. In other words, the frequency of this acoustic wave is $f_a = v_a/\lambda_a = v_a/(\lambda_{Bm}/2)$. The backscattered beam will interfere with the pump beam to form a traveling wave at the difference frequency f_a that propagates along the pump direction. This traveling wave will induce an acoustic wave (via the electro-striction effect in quartz) that propagates along the pump direction and enhances that particular thermal acoustic wave that satisfied the Bragg condition.

With increasing pump intensity, the intensity of the acoustic wave increases, and consequently the intensity of the backscattered beam, i.e., the Brillouin beam, will increase. The growth or the amplification of the Brillouin beam with pump intensity is stimulated Brillouin scattering.[3] The downshift of the Brillouin beam from the pump is therefore $2 f_p v_a/c_m$ and the width of the stimulated Brillouin scattering is determined by the damping of the acoustic waves, i.e., phonon relaxation, in the medium.[4] For a quartz fiber at a λ of 1 micron, the downshift is about 15 GHz and the bandwidth of the SBS is about 25 MHz.

The following describes the operation of the SBS laser.[5]

---

[1] Professor, Rutgers University, New Brunswick, New Jersey.

[2] Professor, Harvard University, Cambridge, Massachusetts.

[3] R.Y. Chiao, C.H. Townes, and B.P. Stoicheff, *Phys. Rev. Lett.* 12: 592 (1964).

[4] D. Heiman, D.S. Hamilton, and R.W. Hellwarth, *Phys. Rev. B* 19: 6583 (1979).

[5] K.O. Hill, B.S. Kawasaki, and D.C. Johnson, *Appl. Opt. Lett.* 28: 608 (1976); D.R. Ponikvar, and S. Ezekiel, *Opt. Lett.* 6: 398 (1981); L.F. Stokes, M. Chodorow, and H.J. Shaw, *Opt. Lett.* 7: 509 (1982).

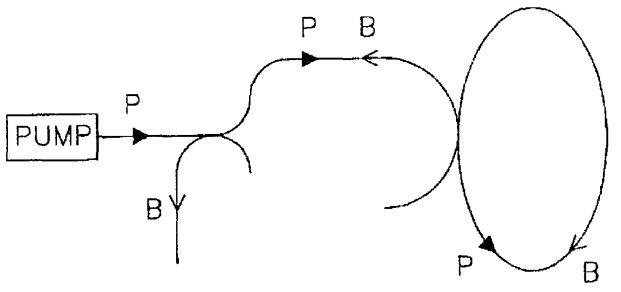

Figure 1. Brillouin laser output.

Figure 1 shows the pump propagating in a fiber ring resonator. If the pump frequency is held at the center of a cavity resonance, the pump intensity inside the resonator is enhanced. The resulting SBS which propagates along the opposite direction of the pump will also be enhanced when there is a cavity resonance within the SBS bandwidth. If the SBS gain in the resonator is greater than the loss, we get SBS lasing as denoted by B in figure 1. Threshold pump power for SBS lasing can be very low, 35 μW, which we recently achieved.[6] The frequency of the SBS laser is therefore determined primarily by the acoustic velocity in the fiber, and the spectral width of the SBS laser can be very narrow,[7] around 1 kHz, since the fiber cavity is a relatively quiet cavity. In this way, the SBS laser linewidth can be much narrower than the pump spectral width.[7] However, if the pump spectral width does not lie well within the passive linewidth of the cavity, we get pump intensity fluctuations within the resonator which will broaden out the SBS laser spectral width.

By constructing two similar Brillouin lasers and subjecting one of them to a disturbance such as temperature, pressure, acoustics, magnetic field, etc., then the beat between the two lasers will give a very sensitive measure in digital form of the applied disturbance.

Since the linewidth of the Brillouin laser can be much narrower than that of the pump laser, the Brillouin laser concept can also be used as a means of reducing the jitter of a laser, especially high frequency jitter, without the need for sophisticated wideband feedback loops.[7]

There are many applications of the two Brillouin lasers that share the same fiber cavity but have either common or independent pumps. Because cavity fluctuations are common to both lasers in this case, the relative jitter between the two lasers is very small. Measuring this relative frequency jitter by simply beating the outputs of two Brillouin lasers that share the same cavity, we found the width of the beat to be limited by the 30 Hz instrumental linewidth of our spectrum analyzer.[7]

Applications of the common cavity Brillouin lasers include:

- fiberoptic ring laser gyroscope, where the output is inherently digital, similar to the HeNe ring laser gyroscope;[6]
- magnetic field sensor with a digital readout;
- tunable, narrow linewidth, high frequency sources in the microwave to millimeter-wave range;[7]
- the generation of high frequency, amplitude modulated laser beams for use in sensitive absolute distance and ranging measurements;[7]
- wideband frequency shifting without the need for wideband modulators;
- the generation of two laser sources with correlated frequency jitter for use in high resolution two-photon interactions for the development of atomic clocks, precision two-photon spectroscopic studies and fast flow laser doppler velocimeters (LDV);[7]
- finally, a distributed spectroscopic sensor based on two-photon interaction using exposed sections of fiber, where the pump photon is pulsed and the probe photon is CW.

[6] F. Zarintechi, S.P. Smith, and S. Ezekiel, *Opt. Lett.* 16: 229 (1991).

[7] S.P. Smith, F. Zarintechi, and S. Ezekiel, *Opt. Lett.* 16: 393 (1991).

1.2 Stimulated Brillouin Fiber Laser Gyroscope

Sponsor

Charles S. Draper Laboratory
Contract DL-H-418468

We present recent developments in a new type of fiberoptic gyroscope[8] based on two counterpropagating stimulated Brillouin lasers[9] sharing the same single mode fiber ring resonator. In the presence of inertial rotation normal to the plane of the resonator, a difference frequency is automatically generated between the counterpropagating Brillouin lasers which is proportional to the rotation, as predicted by the Sagnac effect.[10] The operation of such a gyro is very similar to that of the bulkoptic ring laser gyro (RLG) that is based on two counterpropagating He-Ne lasers that share the same ring resonator.[11] Unlike the passive interferometric fiber gyro,[12] the Brillouin fiber gyro does not require external means for the measurement of nonreciprocal phase shifts induced by the rotation.

Figure 2 shows a simplified schematic diagram of the Brillouin fiber laser gyroscope. Light from a 2 mW single frequency He-Ne pump laser at 1.15 micrometers is split into two beams, P1 and P2, and these beams are frequency shifted by acousto-optic (A/O) modulators before they are coupled along opposite directions of a fiber ring resonator. The fiber resonator is made from a 25 m long single mode fiber wrapped around a cylindrical drum 7.5 cm in diameter. The finesse of the resonator is 250 and the linewidth is 30 kHz. In order to achieve the lowest Brillouin threshold, the polarizations of the input beams are matched into an eigen polarization of the resonator, and the frequency of pump P1 is held at the center of the cavity resonance by a servo loop. When the pump intensities were increased above 60 microwatts, we observed Brillouin lasing, B1 and B2, along directions opposite to those of P1 and P2, that were downshifted by 15 GHz from the pump as expected for the stimulated Brillouin[9] effect at this wavelength. B1 and B2 are combined by beam splitter BS1 and directed to detector D1, after passing through a Fabry-Perot cavity acting as a filter to block out the pump.

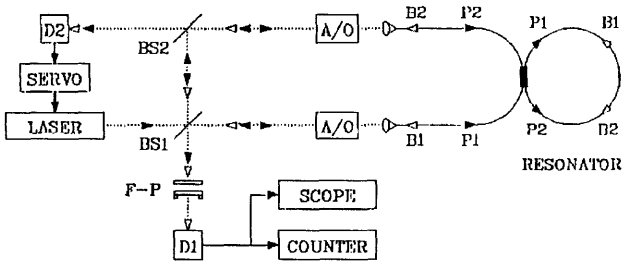

Figure 2.

Figure 3a shows the 3 kHz sinusoidal beatnote between B1 and B2 when a constant rotation of 4 degrees/second is applied to the set up. The magnitude of this beatnote is consistent with that predicted by the Sagnac effect for this configuration and varies linearly with rotation. However, at low rotation rates, the corresponding beatnote becomes highly nonlinear, as shown in figure 3b, and disappears altogether when operating close to zero rotation. This undesirable behavior at low rotation rates, caused by the coupling of the Brillouin lasers through backscattering within the fiber resonator, is called the "lock-in" effect and has been studied extensively in bulkoptic ring laser gyros.

---

[8] S.P. Smith, F. Zarintechi, and S. Ezekiel, "Fiberoptic Ring Laser Gyroscope," *Proceedings of OFS '89,* Paris, France, 1989.

[9] P.J. Thomas, H.M. van Driel, and G.I.A. Stegeman, "Possibility of Using an Optical Fiber Brillouin Ring Laser for Inertial Sensing," *Appl. Opt.* 19: 1906 (1980); K.O. Hill, B.S. Kawasaki, and D.C. Johnson, "Cw Brillouin Laser," *Appl. Phys. Lett.* 28: 608 (1976); D.R. Ponikvar and S. Ezekiel, "Stabilized Single-frequency Stimulated Brillouin Fiber Ring Laser," *Opt. Lett.* 6: 398 (1981); L.F. Stokes, M. Chodorow, and H.J. Shaw, "All Fiber Stimulated Brillouin Ring Laser with Submilliwatt Pump Threshold," *Opt. Lett.* 7: 509 (1982); P. Bayvel and I.P. Giles, "Evaluation of Performance Parameters of Single Mode All Fiber Brillouin Ring Lasers," *Opt. Lett.* 14: 581 (1989).

[10] A.H. Rosenthal, "Regenerative Circulatory Multiple-beam Interferometry for the Study of Light-propagation Effects," *J. Opt. Soc. Am.* 52: 1143 (1962).

[11] W.M. Macek and D.T.M. Davis, Jr., "Rotation Rate Sensing with Traveling Wave Ring Laser," *Appl. Phys. Lett.* 2: 67 (1963).

[12] V. Vali and L.W. Shorthill, "Fiber Ring Interferometer," *Appl. Opt.* 15: 1099 (1976).

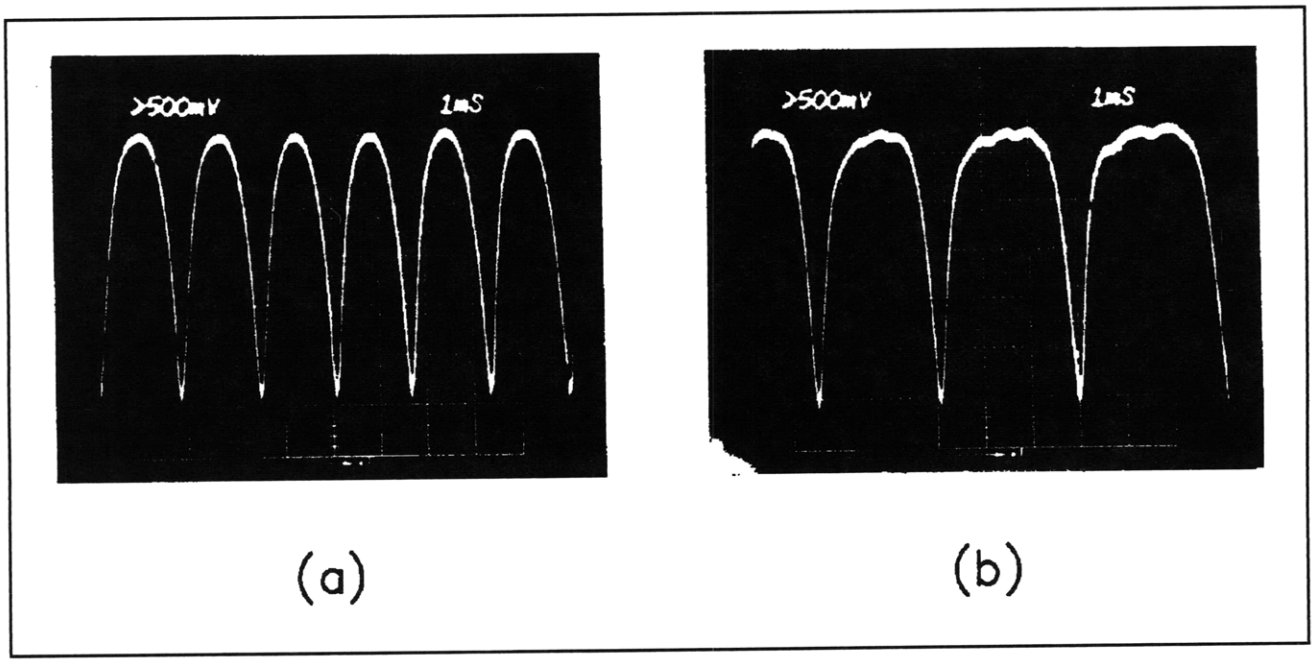

Figure 3.

Figure 4a shows the variation of the Brillouin beatnote, measured by a frequency-to-voltage converter, as a function of an applied sinusoidal rotation, shown in figure 4b, having a peak angular deviation of 5 degrees and a period of 12 seconds. As shown in figure 4a, the Brillouin beat note varies linearly with rotation rate and exhibits a peak beat frequency of 2 kHz for a peak rate of 2.5 degrees/second. However, at low rotation rates, as mentioned above, the beat goes to zero, demonstrating a "lock-in" range of about 1 kHz. To record the direction of the angular motion in figure 4a, a 5 kHz frequency difference was applied to the acousto-optic shifters in figure 2 to generate a bias of 5 kHz. The main advantage of the Brillouin gyro is that it puts an output frequency in response to an applied rotation, without the need for a complicated measurement system.

The data presented here is still preliminary; there are a number of issues that influence performance that have yet to be investigated. For example, a suitable means must be found to overcome the "lock-in" effect. In addition, error sources due to fiber birefringence, back scattering, optical Kerr effect, etc., must be studied. Finally a convenient pump source, preferably a solid state laser such as a semiconductor laser or fiber laser, needs to be identified.

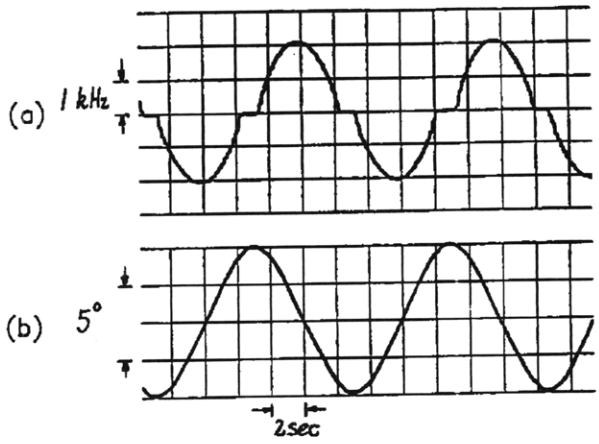

Figure 4.

1.3 Structures Much Shorter and Longer Than Optical Wavelengths Predicted in the Force on a Three-Level System

Sponsor

U.S. Air Force - Electronic Systems Division
Contract F19628-89-K-0030

Recently, a three-level atom in the Λ configuration has been employed to cool atoms in one dimension to the lowest temperature yet achieved. In addition, recent calculations have indicated that structures observed in trapped atoms may be due to interactions with such a system. We have calculated the force on this kind of system excited by Raman resonant bichromatic standing wave light fields in the limit when optical pumping into the trapped state is important.[13] For simplicity, we have considered stationary atoms first. The influence of the non-absorbing trapped state leads to very different predictions for the optical forces than in the case of two level atoms or three level atoms in the Λ configuration. In particular, large stimulated forces can be produced which vary on distance scales both much longer and much shorter than the optical wavelength. Our results differ significantly from those derived in other theoretical treatments[14] which ignore optical pumping into the trapped state.

The appropriate atomic level diagram is shown in figure 5. The basis state transformation is given by:[15]

$$\begin{bmatrix} |-> \\ |+> \\ |e> \end{bmatrix} = \begin{bmatrix} \cos\theta & -\sin\theta & 0 \\ \sin\theta & \cos\theta & 0 \\ 0 & 0 & 1 \end{bmatrix} \begin{bmatrix} |a> \\ |b> \\ |c> \end{bmatrix}$$

where θ is defined by the following Rabi frequency expressions:

$$\Omega_1 = \sqrt{2}\,\Omega \sin\theta = \Omega_0 \sin(kx),$$

$$\Omega_2 = \sqrt{2}\,\Omega \cos\theta = \Omega_0 \sin(kx + \Psi), \text{ and}$$

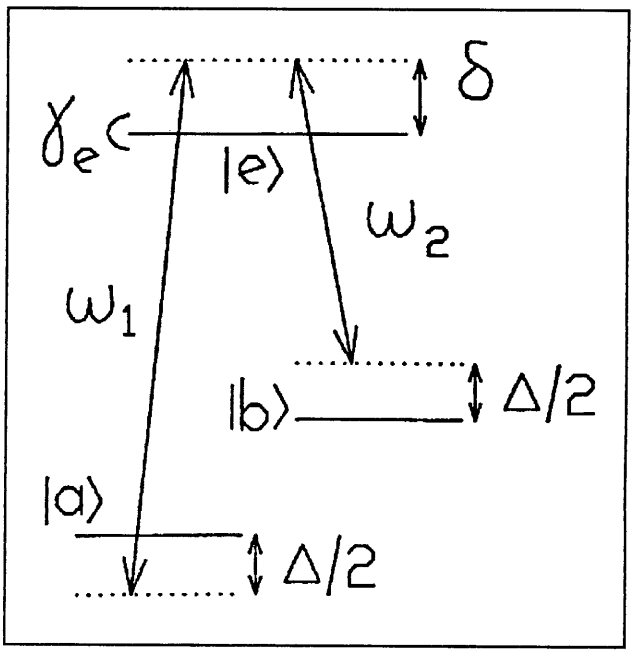

Figure 5. Schematic diagram of a three-level system in the Ω configuration.

$$\sqrt{2}\,\Omega = \sqrt{|\Omega_1|^2 + |\Omega_2|^2}$$

Here, Ψ varies on the scale of the beatlength, which is assumed negligible on the optical wavelength scale.

For zero difference detuning $\Delta \neq 0$, the $|->$ state is coupled to the $|+>$ state and both states experience a force. We find that this force is proportional to Δ and can be separated into a component associated with the $|+>$ state and a component associated with the $|->$ state. The $|+>$ state component averages to zero over an optical wavelength while the $|->$ state component can have a substantial non-zero average value. An example of this is shown in figure 6 for the $\delta = 0$ case where the $|+>$ state force is zero. This rectified component of the force (dashed line in figure 6) is periodic over half the beat wavelength as shown in figure 7. It is important to note that the force also displays features which are much narrower than an optical wavelength (see figure 6). Further calculations are needed to determine the implications of these narrow structures.

---

[13] M.S. Shahriar, P.R. Hemmer, N.P. Bigelow, and M.G. Prentiss, *Proceedings of the Quantum Electronics and Laser Science Conference,* Baltimore, Maryland, 1991.

[14] J. Javanainen, *Phys. Rev. Lett.* 64: 519 (1990).

[15] H.R. Gray, R.M. Whitley, and C.R. Stroud, Jr., *Opt. Lett.* 3: 218 (1978).

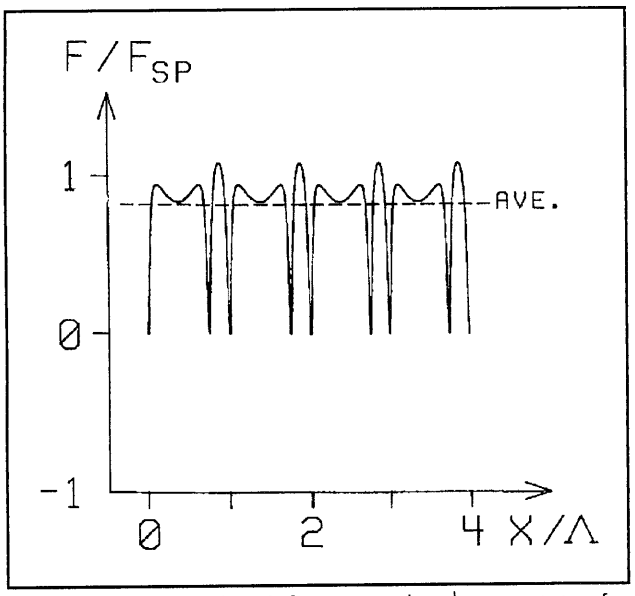

Figure 6. Stimulated force on the $|->$ state, for $\delta = 0$, $2\Delta = \Omega_0 = 4\gamma_0$, $\Psi = \pi/4$. Dashed line is average (rectified) force.

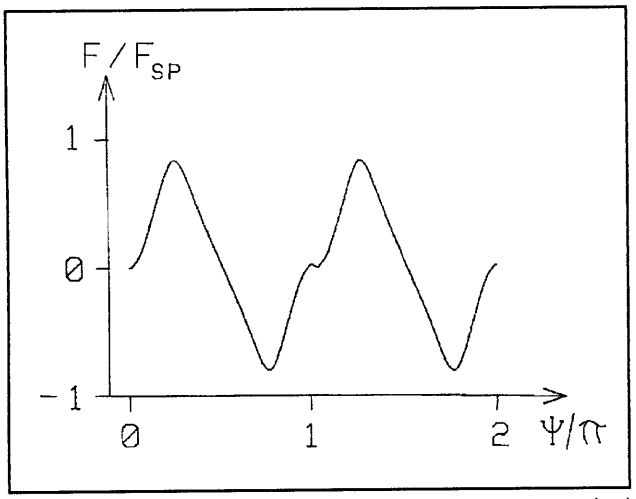

Figure 7. Rectified force, averaged over an optical wavelength, plotted as a function of Ψ, over one beat wavelength, for $\delta = 0$, $2\Delta = \Omega_0 = 4\gamma_0$.

1.4 Phase-Locked, Closed-Loop Three-Wave Mixing Demonstrated in Atomic Sodium via Excitation of Microwave Dressed States With Optical Frequencies

Sponsor

U.S. Air Force - Electronic Systems Division
Contract F19628-89-K-0030

It is well known[16] that a laser excited Raman interaction causes atoms to be optically pumped into a non-absorbing dressed state called the trapped state. In atomic sodium, the trapped state consists of a linear combination of hyperfine levels having a microwave frequency separation. We have demonstrated that in the presence of a resonant microwave field, the Raman trapped state translates into one or the other microwave spin-locked (dressed) state under appropriate experimental conditions.[17] Analogously, we have shown that a microwave field can also be used to excite the optical Raman trapped state.

Figure 8a shows a three-level atomic system in the Λ configuration where ω_1 and ω_2 are the frequencies of the optical fields and ω_3 is the frequency of the microwave field. Here it is assumed that states 1 and 3 are long lived, but state 2 is short lived with a decay rate of γ_2. The Raman trapped state has the form[16]

$$|1> |n_1 + 1> |n_2> \exp(i(k_1 z_1 - k_2 z_2)) -$$

$$|3> |n_1> |n_2 + 1>,$$

where equal Rabi frequencies have been assumed. Here, $|1>$ and $|3>$ are the bare-atom states, and $|n_1> |n_2>$ is a field state with n_1 photons at frequency ω_1 and n_2 photons at ω_2. In addition, $(k_i z_i)$ represents the phase of the field at frequency ω_i, and the phase factor of the field at ω_2 has been factored out. Similarly, the high- and low- energy dressed states of the ground sublevel microwave transition[18] are

---

[16] H.R. Gray, R.M. Whitley, and C.R. Stroud, Jr., *Opt. Lett.* 3: 218 (1978); G. Alzetta, A. Gozzini, L. Moi, and G. Orriols, *Nuovo Cimento 36B: 5 (1976).*

[17] M.S. Shahriar and P.R. Hemmer, *Phys. Rev. Lett.* 65: 1277 (1985).

[18] S.R. Hartmann and E.L. Hahn, *Phys. Rev.* 128: 2042 (1962); Y.S. Bai, A.G. Yodh, and T.W. Mossberg, *Phys. Rev. Lett.* 55: 1277 (1985).

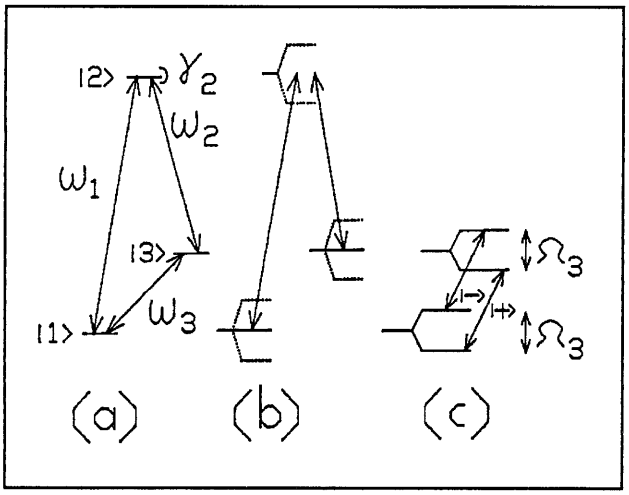

Figure 8.

$$|1> |n_3 + 1> \exp(i(k_3 z_3)) - |3> |n_3>$$

and

$$|1> |n_3 + 1> \exp(i(k_3 z_3)) + |3> |n_3>$$

respectively.

To help clarify the physics involved, consider a step-wise process wherein the optical Raman interaction and the microwave interaction are separated in time. First, the optical Raman interaction puts the atoms into the trapped state as illustrated in figure 8b. Next, the laser fields are turned off and a microwave field is turned on. In general, two microwave dressed states are possible as shown by the energy level diagram of figure 8c. To determine into which microwave eigenstate the Raman trapped state evolves, it is necessary to know the relative phase of the microwave and the double optical (Raman) fields. This relative phase is given by

$$\phi = [(k_1 z_1 - k_2 z_2) - k_3 z_3],$$

where it is assumed that all three states are in phase at

$$z_1 = z_2 = z_3 = 0.$$

When the laser difference frequency is exactly in (or out of) phase with the microwave frequency, i.e., $\phi = 0$ (or $\phi = \pi$), the Raman trapped state translates directly into the high (or low) energy microwave dressed state. For any other value of the relative phase ϕ, a linear combination of microwave dressed states results. In such a case, Rabi spin flips occur (>) (largest for $\phi = \pi/2$), partially destroying the original dressed state. To detect the degree of microwave interaction, the microwave field can be turned off, and the Raman interaction can be turned back on. Population lost from the trapped state would then appear as an increase in optical absorption.

Experimentally, the three-step process can be realized using a separated field excitation scheme in an atomic beam. The experimental setup we used is illustrated schematically in figure 9. To minimize the effects of laser jitter,[19] the field at frequency ω_2 is generated from that at ω_1 by using an acousto-optic modulator (A/O). The microwave field is generated by detecting and amplifying the beat between the two optical fields using a 2 GHz avalanche photodiode (APD). This ensures that the microwave and the double optical fields are phase locked. The relative phase ϕ between the microwave and laser difference frequencies is controlled with an optical delay line consisting of a translating corner cube (as shown in figure 9).

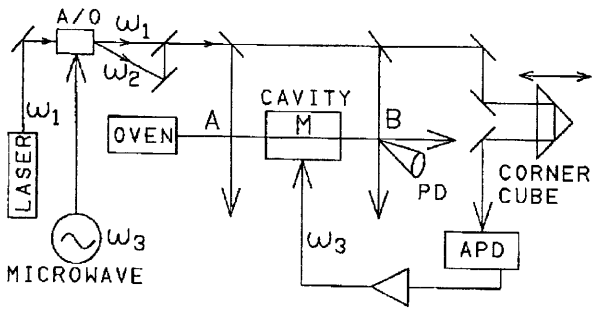

Figure 9.

First, Raman excitation in zone A pumps the atoms into the trapped state. Then, these atoms interact with a microwave field, zone M. The Raman probing interaction in zone B measures the degree of the microwave interaction by detecting any loss of the trapped state population, via the fluorescence detecting photodiode (PD). The pathlengths to zones A and B are set so that the optical difference frequencies in zones A and B are in phase.

Figure 10a shows the Raman-Ramsey fringes observed in zone B when the laser difference is scanned, for zero microwave power. Figure 10b shows the fluorescence observed, with the laser

[19] N.F. Ramsey, *Molecular Beams* (London: Oxford University Press, 1956); J.E. Thomas, P. R. Hemmer, S. Ezekiel, C.C. Leiby, Jr., R.H. Picard, and C.R. Willis, *Phys. Rev. Lett.* 48: 867 (1981).

difference frequency held exactly on resonance (fluorescence minimum), but the microwave power scanned. Here, the microwave field is exactly in phase with the optical difference frequency, i.e., $\phi = 0$. As can be seen, the microwave field has no effect, since in this case the optical Raman trapped state translates into a pure microwave spin-locked eigenstate. Figure 10c shows the case of $\phi = \pi/2$, as the microwave power is scanned again with the laser difference frequency held on resonance. Here, the fluorescence depends strongly on microwave power, undergoing large oscillations caused by Rabi spin flips, indicating that a microwave eigenstate is no longer excited. The damping with increasing microwave power in figure 10c is caused by velocity averaging effects. Comparison with the theoretical plots of figures 10d, 10e, and 10f show good agreement.

We also performed the complimentary experiment in which a microwave field is used to excite the optical Raman trapped state. This involves replacing the first Raman zone in figure 9 by an optical pumping zone (not shown), which effectively puts all the atoms into state $|3>$ before entering the microwave cavity. For a microwave power corresponding to a $\pi/2$ pulse, the resulting state is

$$(-i|1>|n_3>\exp(-ik_3z) + |3>|n_3 - 1>)$$

This can be made to correspond to a Raman trapped state if the relative phase ϕ between the microwave and the laser difference frequency is $\pi/2$.

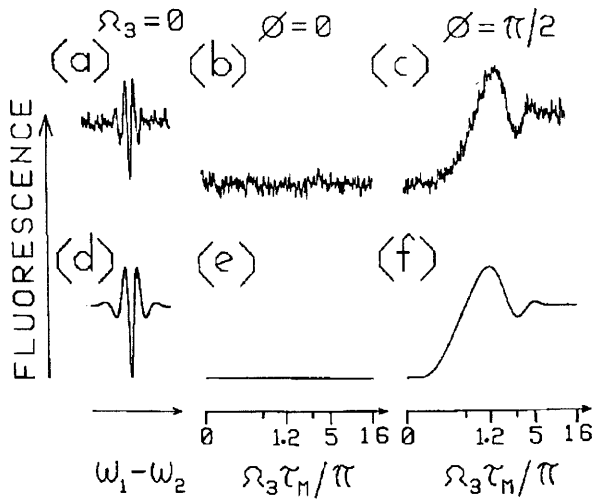

Figure 10.

Experimental evidence of microwave excitation of an optical Raman trapped state appears in figure 11. Figure 11a shows the zone B fluorescence obtained by scanning the laser difference frequency with a microwave power corresponding to a $\pi/2$ pulse and a relative phase of $\phi = \pi/2$. As can be seen, Ramsey fringes are obtained which closely resemble those in figure 10a, even though only one Raman excitation zone is present. Thus, an optical Raman trapped state has been excited by the microwave field. For completeness, figure 11b shows the zone B fluorescence obtained with the microwaves turned off. As expected, no Ramsey fringes are seen in this case.

Extension of these results to a single zone excitation scheme (where both microwave and optical Raman fields are present simultaneously) is also of interest because of the possibility of exciting a three photon trapped state. This would occur for a relative Raman and microwave phases of $\phi = 0$ or π. For other values of ϕ, all dressed states are partially optically absorbing, where the steady state absorption depends on ϕ. For a properly chosen configuration, the position dependence of the relative phase ϕ would result in a grating being produced, which would diffract both optical and microwave fields. Numerous applications of this effect can be imagined if the microwave transition is replaced by a mm-wave or far infrared transition. For example, real time mm-wave beam steering can be performed wherein the mm-wave could be deflected by the optical beams. It should also be possible to perform real time holographic far infrared to visible image conversion.

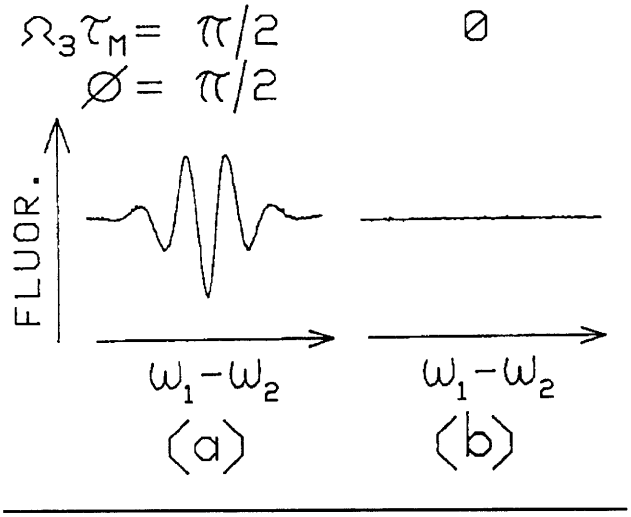

Figure 11.